

Self-organization in the static pair annihilation process

This article has been downloaded from IOPscience. Please scroll down to see the full text article.

1995 J. Phys. A: Math. Gen. 28 5165

(<http://iopscience.iop.org/0305-4470/28/18/008>)

View [the table of contents for this issue](#), or go to the [journal homepage](#) for more

Download details:

IP Address: 171.66.16.68

The article was downloaded on 02/06/2010 at 00:28

Please note that [terms and conditions apply](#).

Self-organization in the static pair annihilation process

B Bonnier†§, R Brown† and E Pommiers†

† Centre de Physique Théorique et de Modélisation, UA 1537 du CNRS, Université Bordeaux I, 19 rue du Solarium, F 33175 Gradignan Cedex, France

‡ Centre de Physique Moléculaire Optique et Hertzienne, UA 283 du CNRS, Université Bordeaux I, F 33405 Talence Cedex, France

Received 13 April 1995

Abstract. The pair annihilation of identical particles initially distributed at random, and interacting by a tunnelling law is studied. Monte Carlo simulations are performed in one and two dimensions to measure the density and the two-particle correlations which show a tendency to local ordering of the surviving particles. This model is shown to be equivalent to a simpler model that we can solve on a one-dimensional lattice. In this case, the self-ordering property can be proved and characterized. This analysis is then naturally extended to higher dimensionalities.

1. Introduction

Disordered systems submitted to stochastic dynamics can show a tendency to self-organization [1]. This is well known for open systems involving nonlinear dissipative transport which evolve into a self-organized critical state [2]. More generally, dynamical long-range correlations can be expected in non-equilibrium steady states. Long-range (compared to the initial separation) correlations may also arise in static and diffusing reaction systems from the interplay of a time-dependent reaction front (defined below) with fluctuations in the initial distribution of reactants [3–5]. Here, we are specifically concerned with the kind of self-organization which is found to appear in the large time regime of static pair annihilation (SA) processes.

In this model a set of A particles randomly distributed on a lattice remain fixed and are removed by fusion, $A + A \rightarrow 0$, with an isotropic rate $w(r) = w_0 \exp(-r/r_0)$ for any two particles separated by distance r . Monte Carlo (MC) simulations on a cubic lattice clearly indicate the growth with time of the two-particle correlation function $g_2(r, t)$ [6]. Mean field theory thus fails to predict the surviving particle density $\rho(t)$ at long times, which is found to decrease in a universal way, and is related to the space dimension and not to the initial distribution.

Our aim here is to give some analytical insight into the dynamical generation of the observed order. In addition, this allows us to give an accurate description of the decay at any time. This is useful from a practical point of view: $\rho(t)$ is, for example, directly linked to delayed fluorescence in disordered solid solutions of aromatic molecules, the $A + A \rightarrow 0$ reaction corresponding to fusion in triplet states [7].

The way we proceed is to consider a simpler model where the annihilation is constrained to occur through a cascade of successive stages, each stage corresponding to a fixed value

§ E-mail address: Bonnier@bortibm1.in2p3.fr

of the interaction range. In the first stage, all pairs of neighbours are randomly destroyed, in the second stage, all pairs of next-to-nearest neighbours vanish, and so on. Within each stage the dynamics is simple, the difficulty being how to keep track of the initial data entering any stage which are given by the configuration of the system at the end of the previous stage.

As we show in the next section, this staggered static annihilation (SSA) model can be exactly solved on a one-dimensional lattice, in contrast to the SA model. Its long-range order appears as a consequence of the re-summation of the fluctuations on any scale. In order to compare these exact results with the SA model, we have performed MC simulations of the SA process on a line and on a one-dimensional lattice. This is done in section 3 where we show the asymptotic equivalence of the two models and propose a mapping between the SA and SSA models at any time.

From the analysis of the self-ordering in one dimension, we expect an analogous dynamical clustering to occur in higher dimensions; this is explained in section 4 where we discuss MC simulations of the SA model in two and three dimensions.

2. Exact solution of the SSA model

We precisely define the SSA model in the following way. Consider a set of particles on sites of an infinite one-dimensional lattice of unit spacing. Initially, the sites are randomly and uniformly occupied with at most one particle per site, at some arbitrary particle density ρ_0 . Then, the particles decay through the static staggered pair annihilation described in section 1. By definition, the decay is such that at any stage no particle can survive between the two members of an annihilating pair. Any surviving particle thus separates the lattice into left and right uncorrelated sub-lattices. This screening property is at the root of the solvability of the model.

We first solve the dynamics during an arbitrary stage that we label j , $j \geq 1$. To describe the random sequential decay during this stage, we introduce an internal time τ_j and the more convenient variable $z = e^{-\tau_j}$ which runs from one (beginning of the stage) to zero (end of the stage = complete disappearance of the pairs involved). Let $\rho(z)$ be the density and $P(r_1, \dots, r_{n-1}; z)$ the probability of observing at time z (within stage j) a string of n particles with separations r_1, \dots, r_{n-1} in the lattice spacing unit. The screening property allows us to write

$$P(r_1, \dots, r_{n-1}; z) = \rho(z) \prod_{i=1}^{n-1} \gamma(r_i; z) \quad (2.1)$$

where $\gamma(r, z)$ is a conditional probability normalized according to $\gamma(0, z) = 1$. Clearly, $\rho(z)$ and $\gamma(r, z)$, linked to the pair probabilities $P(r; z)$, are sufficient to describe the configurations. We recall that $\gamma(r, z) = 0$ for $1 \leq r < j$ since we are in stage j , and since only pairs with separation j interact, we have the master equations

$$\begin{aligned} z \partial_z \rho(z) &= 2P(j; z) \\ z \partial_z P(j; z) &= P(j; z) + 2P(j, j; z) \\ z \partial_z P(r; z) &= 2P(j, r; z) + 2P(j, r - j; z) \quad r > j \end{aligned} \quad (2.2)$$

of which the right-hand sides show the various ways of destroying a particle. For example, the factor $2P(j; z)$ in the first equation is the probability that a particle annihilates with a right or left neighbour at distance j . The second equation describes the evolution of the probability of a pair with separation j : the members of the pair can annihilate mutually with

probability $P(j; z)$, or each member can annihilate with a third particle at distance j , which gives the additional factor $2P(j, j; z)$. If the separation r of the pair is greater than j , the annihilation necessarily involves a third particle. This particle can be external, which gives a probability $2P(j, r; z)$, or located between the two members of the pair, which gives a probability $2P(j, r - j; z)$, as indicated in the third equation. Using (2.1) with $n = 2$, one obtains

$$z\partial_z\rho(z) = 2\rho(z)\gamma(j; z) \quad z\partial_z\gamma(j; z) = \gamma(j; z) \quad z\partial_z\gamma(r; z) = 2\gamma(j; z)\gamma(r - j; z) \tag{2.3}$$

and thus

$$\rho(z) = \rho(1)e^{2(z-1)\omega_j} \tag{2.4}$$

$$\gamma(j; z) = z\omega_j \tag{2.5}$$

where we have introduced a stage factor $\omega_j = \gamma(j; z = 1)$ to be determined below. To solve for $\gamma(r, z)$, it is convenient to consider the generating function

$$\Gamma(x; z) = \sum_{r \geq 1} x^r \gamma(r; z) = x^j z \omega_j + \sum_{r > j} x^r \gamma(r; z) \tag{2.6}$$

which from (2.3) fulfils $\partial_z \Gamma(x, z) = x^j \omega_j \{1 + 2\Gamma(x; z)\}$.

One thus obtains

$$1 + 2\Gamma(x; z) = e^{2(z-1)\omega_j x^j} \{1 + 2\Gamma(x; 0)\}. \tag{2.7}$$

We are now in a position to sum up all the stages. Our conventions are to write ρ_{j-1} for the density at the beginning of the stage j (and thus ρ_0 is the initial density) and ρ_j at the end. From equation (2.4) one has with $z = 0$, $\rho_j = \rho_{j-1}e^{-2\omega_j}$ and thus

$$\rho_j = \rho_0 \exp\left(-2 \sum_{k=1}^j \omega_k\right). \tag{2.8}$$

In the same way, $\Gamma_{j-1}(x)$ and $\Gamma_j(x)$ denote the pair probability functional at the beginning and at the end of the stage j . Equation (2.7) then reads

$$1 + 2\Gamma_j(x) = e^{-2x^j \omega_j} \{1 + 2\Gamma_{j-1}(x)\}$$

and thus

$$1 + 2\Gamma_j(x) = \exp\left(-2 \sum_{k=1}^j x^k \omega_k\right) \{1 + 2\Gamma_0(x)\} \tag{2.9}$$

where the initial $\Gamma_0(x)$ is given by

$$\Gamma_0(x) = \sum_{r \geq 1} x^r \rho_0 = \frac{x\rho_0}{1-x}$$

since the distribution is uniform.

Relation (2.9) can be rewritten as

$$2 \sum_{k=1}^j x^k \omega_k = \ln\left(\frac{1 - (1 - 2\rho_0)x}{1 - x}\right) - \ln(1 + 2\Gamma_j(x)) \tag{2.10}$$

where $\Gamma_j(x)$ behaves like x^{j+1} as $x \sim 0$ (equation (2.6) with $z = 0$), and thus

$$\sum_{k=1}^j x^k \omega_k = \frac{1}{2} \ln\left(\frac{1 - (1 - 2\rho_0)x}{1 - x}\right) + O(x^{j+1}). \tag{2.11}$$

Identification of the powers of x on either side of (2.11) gives the stage factors ω_k :

$$\omega_k = \frac{1 - (1 - 2\rho_0)^k}{2k} \quad k \geq 1 \quad (2.12)$$

which completes the determination of the model at stage j in terms of the initial data.

Returning to the density ρ_j , we write $\rho_j = \rho_0 \exp(-\sum_j)$ with

$$\sum_j \equiv \sum_{k=1}^j \frac{1 - (1 - 2\rho_0)^k}{k} = \int_{1-2\rho_0}^1 \frac{du}{1-u} \frac{1-u^j}{1-u}$$

which gives its continuation to any positive real value of j and its asymptotic behaviour as $j \rightarrow +\infty$. Putting $u = 1 - v/j$ in the last integral, one finds

$$\sum_j \sim \int_0^{2\rho_0 j} dv \frac{1 - e^{-v}}{v} \sim \gamma + \ln(2\rho_0 j)$$

where $\gamma = 0.577215\dots$ is the Euler constant. The 'universal' asymptotic behaviour of the density is thus

$$\lim_{j \rightarrow \infty} \rho_j = \frac{e^{-\gamma}}{2j}. \quad (2.13)$$

The two-particle correlation function at distance r , $g_j(r)$, is given by

$$g_j(r) = \frac{\rho_j^{-1}}{r!} \left. \frac{d^r}{dx^r} \Gamma_j(x) \right|_{x=0}$$

where $1 + 2\Gamma_j(x) = \exp(2 \sum_{k \geq j+1} x^k \omega_k)$. This last relation is just equation (2.9) where (2.12) has been used. One finds, for example,

$$\begin{aligned} g_j(r) &= 0 & \text{for } 1 \leq r \leq j \\ g_j(r) &= \rho_j^{-1} \omega_r & \text{for } j+1 \leq r \leq 2j+1 \\ g_j(r) &= \rho_j^{-1} \left\{ \omega_r + \sum_{k=j+1}^{r-j-1} \omega_k \omega_{r-k} \right\} & \text{for } 2j+2 \leq r \leq 3j+2. \end{aligned} \quad (2.14)$$

In the asymptotic regime $j \rightarrow \infty$, it is convenient to rescale the distance $r = j\bar{r}$ where \bar{r} is fixed. In this regime, the correlation function reaches a limiting function $g_\infty(\bar{r})$ given by

$$\begin{aligned} 0 \leq \bar{r} < 1 & \quad g_\infty(\bar{r}) = 0 \\ 1 \leq \bar{r} \leq 2 & \quad g_\infty(\bar{r}) = \frac{e^{\bar{r}}}{\bar{r}} \\ 2 \leq \bar{r} \leq 3 & \quad g_\infty(\bar{r}) = \frac{e^{\bar{r}}}{\bar{r}} \{1 + \ln(\bar{r} - 1)\} \end{aligned} \quad (2.15)$$

and so on. At $\bar{r} = 3$, $g_\infty(\bar{r}) \approx 1.0052$ and the asymptotic \bar{r} limit ($g_\infty(\bar{r} = \infty) = 1$) is practically reached, but the behaviour of $g_\infty(\bar{r})$ between one and three clearly indicates the presence of some order which will be discussed in section 4.

3. The SA model

We recall that in the SA model, a set of A particles are randomly distributed on a lattice, they remain fixed and are removed by fusion, $A + A \rightarrow 0$, with an isotropic rate $w(r) = w_0 \exp(-r/r_0)$ for any two particles separated by distance r . The dynamics of the SA model obey a hierarchy of equations for the n -particle distribution functions [8]. We give the first equations for a one-dimensional lattice, their generalization being straightforward:

$$-\frac{d\rho(t)}{dt} = 2 \sum_{r \geq 1} w(r) \rho_2(r, t) \quad (3.1)$$

$$-\frac{d\rho_2(r, t)}{dt} = w(r) \rho_2(r, t) + 2 \sum_{1 \leq r' < r} w(r') \rho_3(r', r - r', t) + 2 \sum_{r' \geq 1} \{w(r') + w(r + r')\} \rho_3(r, r', t) \quad (3.2)$$

where $\rho_2(r, t)$ and $\rho_3(r_1, r_2, t)$ denote, respectively, the configurationally averaged probabilities at time t for a pair of particles separated by r , and for a triplet with successive separations r_1 and r_2 .

From previous work [6], it appears that standard approximations of this hierarchy, like the Kirkwood approximation [9], are not appropriate for the SA model, except in its initial regime where the mean-field (MF) approximation works. In the MF approximation, one puts $g_2(r, t) = 1$, where the two-particle correlation function $g_2(r, t)$ is linked to $\rho_2(r, t)$ through $\rho_2(r, t) = \rho^2(t) g_2(r, t)$. The formal integration of (3.1) for the density $\rho(t)$, which is

$$\rho(t) = \frac{\rho(0)}{1 + \rho(0) \int_0^t \overline{g_2(t')} dt'} \quad \overline{g_2(t)} = 2 \sum_{r \geq 1} w(r) g_2(r, t) \quad (3.3)$$

then reads

$$\rho_{\text{MF}}(t) = \frac{\rho(0)}{1 + \lambda \rho(0)t} \quad \lambda = \frac{2w_0 e^{-1/r_0}}{1 - e^{-1/r_0}}. \quad (3.4)$$

On the other hand, it has been noticed in simulations of the SA model [6], and as we observe in all our cases, that the two-particle correlation vanishes for separations smaller than the reaction radius $r_a(t)$, which one can define as

$$w(r_a(t))t = 1 \quad r_a(t) = r_0 \ln w_0 t. \quad (3.5)$$

The idea of the reaction front is useful because of the fast radial decay of the interaction, and it can be traced back to work on electron scavenging [10]. The probability of a pair of particles separated by less than $r_a(t)$ is very low. The time t_0 such that $r_a(t_0) \sim 1$ then gives the upper limit where the MF approximation is valid. At that time, the density $\rho(t)$ reaches a value close to the MF value, and for $t \gg t_0$

$$g_2(r, t) = 0 \quad \text{for } r \leq r_a(t). \quad (3.6)$$

Relation (3.6) is, of course, reminiscent of the basic property of the SSA model given in equation (2.14), i.e. $g_j(r) = 0$ for $r \leq j$. The appearance of a regime where (3.6) holds gives an opportunity to use the SSA model to describe the SA model under the identification

$$j \longrightarrow j(t) = r_a(t) \quad (3.7)$$

at least asymptotically.

Then, under the phenomenological assumption (3.7) that the range of interaction at step j of the SSA model is the reaction radius of the SA model at time t , one would obtain,

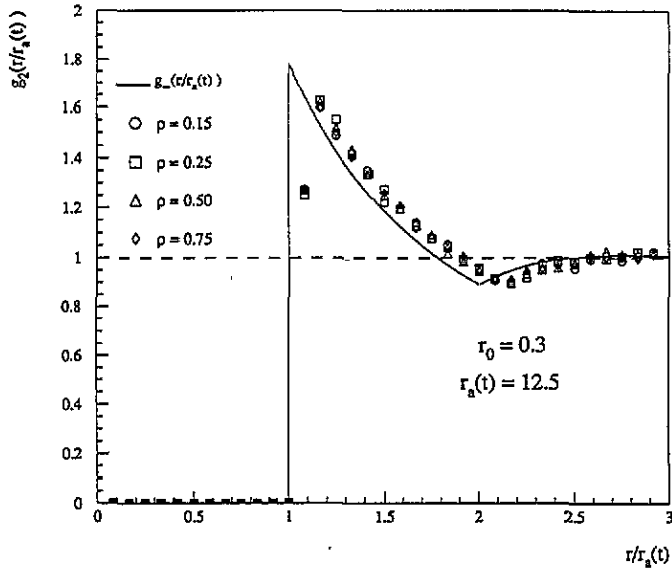


Figure 1. The two-particle correlation at long time (scaled variable $\bar{r} = r/r_a(t)$) in the SA model. The symbols correspond to the MC data obtained for the highest value of $r_a(t)$ ($r_a(t) = 12.5$) on a one-dimensional lattice for various initial densities ρ and the value $r_0 = 0.3$. Data for $r_0 = 0.5$ are of the same kind. The curve is the asymptotic ($r_a(t) = \infty$) correlation as predicted by equation (2.15) from the SSA model. Errors are smaller than the symbols.

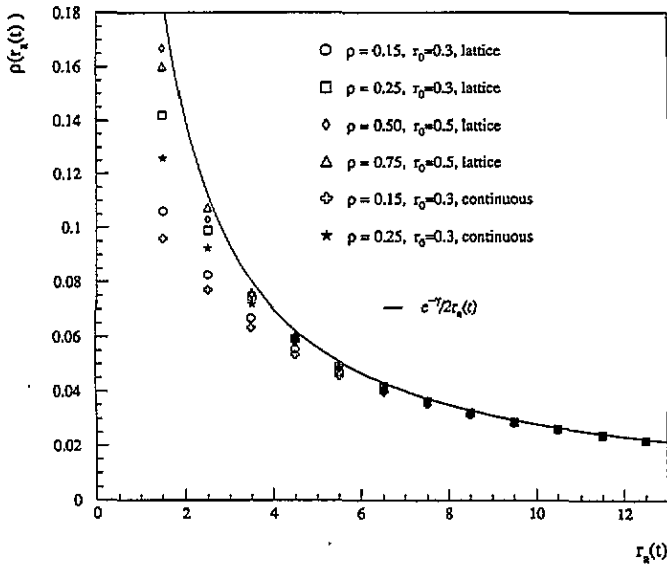


Figure 2. The surviving density $\rho(t)$ as a function of $r_a(t)$ in the SA model. The symbols correspond to the various indicated one-dimensional MC simulations. The curve is the universal asymptotic limit of $\rho(t)$ as predicted by equation (2.13) with $j = r_a(t)$. Errors are smaller than the symbols.

for the asymptotics of the SA, model expression (2.13) for the density, with $j = r_a(t)$ and (2.14) for the two-particle correlation function $g_{\infty}(\bar{r})$, with $\bar{r} = r/r_a(t)$.

These predictions are found to be in perfect agreement with the data derived from the MC simulations, as can be checked from figures 1 and 2. Each set of data corresponds to a sample of 2000 runs, using the algorithm described in [6], on a lattice or a line of 10 000 units length containing from 1500 to 7500 particles, depending on the initial density ρ .

In fact, the identification is not only asymptotic, and a suitable mapping between the parameters of the two models can be performed so as to allow a good fit of the SA model in the whole time regime $t > t_0$ where t_0 is the end of the MF period.

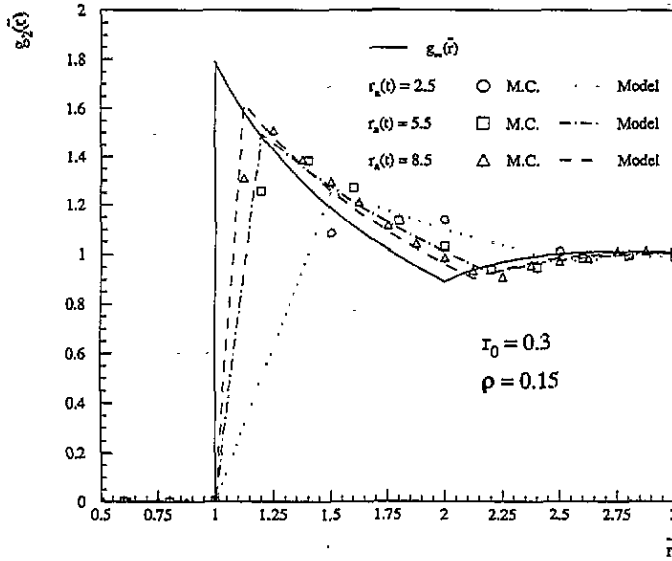


Figure 3. The two-particle correlation function at fixed times. The symbols correspond to the MC simulation on the one-dimensional lattice of the SA model with $\rho = 0.15$, $r_0 = 0.3$. The pair correlation function $g_2(\bar{r})$ is measured at three fixed values of $r_a(t)$ and plotted in the scaled variable $\bar{r} = r/r_a(t) - \frac{1}{2}$. The lines illustrate the corresponding predictions from the SSA model under the mapping of equations (3.8) and (3.9). Errors are smaller than the symbols.

At this point, the continuous and the lattice cases may be distinguished. On the lattice, one can observe from the MC data that one can find a sequence of times t_N , $N \geq 1$ where $N < r_a(t_N) < N + 1$, such that practically all the pairs up to the distance N have been destroyed, the remaining pairs being unaffected. This is a sequence of snapshots where the SA and SSA models can be identified though $j = N$. The precise determination of t_N depends upon the values chosen for the parameters of the SA model. Here, for simplicity, we choose $r_a(t_N) = N + \frac{1}{2}$ and define the mapping

$$j \rightarrow j(t_N) = N = r_a(t_N) - \frac{1}{2} \quad N \geq 1 \tag{3.8}$$

in agreement with the asymptotic constraint (3.7). To complete the determination of the SSA model we have to give its initial density ρ_0 . The end t_0 of the MF period for the SA model must correspond to some $r_a(t_0)$ value between zero and one. We find that $r_a(t_0) = 1 + r_0 \ln \rho_0$, which gives, using (3.4),

$$\rho_{MF}(t_0) = \rho(0) \left[1 + \frac{2r_0\rho(0)}{1 - e^{-1/r_0}} \right]^{-1}$$

as a good choice. The assumption that for $t > t_0$, the dynamics of the SA model can be described by the SSA model for $j \geq 1$, submitted to (3.8), leads us to define the initial density ρ_0 as

$$\rho_0 = \rho_{MF}(t_0). \quad (3.9)$$

Under the correspondence of (3.8) and (3.9) there is, then, a time sequence t_N where the two models coincide. One can check the accuracy of this approximation in figures 3 and 4 where we display the pair correlation and the density. If we extrapolate relation (3.8) to any time t , $t > t_0$, the SSA model remains defined (j real), but it does not necessarily reproduce the details of the SA model within the period $[t_N, t_{N+1}]$. In the SA model the density, for example, can have some r_0 -dependent structure in this interval (see [6]). If necessary, these details can be modelled by a mapping of stage $j = N + 1$ on to period $[t_N, t_{N+1}]$, which involves, in particular, the adjustment of the time constant τ_{N+1} . The physical basis of the mapping is the sharp radial decay of the reaction rate. On average, in the SA process, particles must annihilate with their current nearest neighbours.

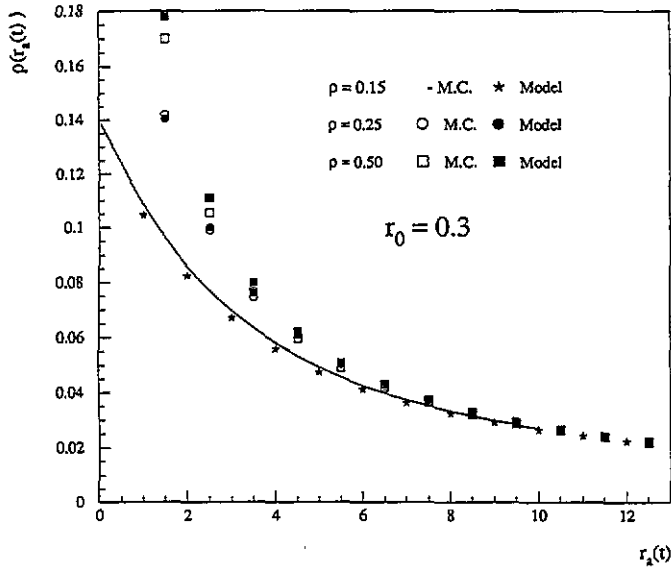


Figure 4. The surviving density $\rho(r)$. A set of three MC experiments is displayed with their corresponding fits by the mapped SSA model. The initial density $\rho = 0.15$ corresponds to the continuous model, the remaining densities, $\rho = 0.25$ and $\rho = 0.50$, correspond to the lattice case. Errors are smaller than the symbols.

We now turn to the continuous case, which is simpler. The end of the MF period can be defined though $r_a(t_0) = 0^+$ and, thus, we define ρ_0 through (3.9) with

$$\rho_{MF}(t_0) = \rho(0)[1 + 2r_0\rho(0)]^{-1}$$

which is given by expression (3.4) in the MF approximation of the continuous SA model ($\lambda = 2w_0r_0$). As there is no 'quantification' of the reaction radius we just take $j \rightarrow j = r_a(t)$ in accordance with the asymptotic relation (3.7) and the boundary condition $j = 0$ for $t = t_0$. A typical fit obtained in this way for the density is shown in figure 4.

4. Nature of the ordering

In one dimension, the self-ordering property of the SA model can be analysed through the SSA model. The asymptotic density is $\rho \sim e^{-\gamma}/2r_a(t)$ and the correlation $g_{\infty}(\bar{r})$ is given by equation (2.15), where \bar{r} is the scaled separation $\bar{r} = r/r_a(t)$. On its first period $0 \leq \bar{r} < 1$, $g_{\infty}(\bar{r}) = 0$, which just reflects an excluded volume effect: because of the sharp drop in $w(r)$ with increasing separation, it is extremely unlikely that two particles survive at a distance less than $r_a(t)$ at time t . A first approximation to the distribution of surviving particles would be to represent them by hard rods (or disks or spheres in higher dimensions) of radius $r_a(t)/2$. In one dimension, the coverage θ associated with this distribution is $\theta = \rho r_a(t) = e^{-\gamma}/2 = 0.2807\dots$. The behaviour of $g_{\infty}(\bar{r})$ for $\bar{r} \geq 1$ reveals the presence of a dynamical clustering, whose short range ($\bar{r} \sim 2$) is reminiscent of the minimal order found in the random sequential adsorption (RSA) of hard rods. It is thus tempting to compare it with the RSA correlation at coverage θ . Using the exact results given in [11], it appears that the SA model self-ordering is stronger than the RSA self-ordering. It is even stronger than the order found in an equilibrium configuration of hard rods at this coverage, since we find for example $g_{\text{RSA}}(\bar{r} = 1, \theta \simeq 0.28) \simeq 1.3$ and $g_{\text{eq}}(\bar{r} = 1, \theta \simeq 0.28) \simeq 1.38$, compared to $g_{\infty}(\bar{r} = 1) \simeq 1.78$. In fact, the best representation of short-range SA order can be given in terms of an RSA model with cooperative effects which enhances clustering [12].

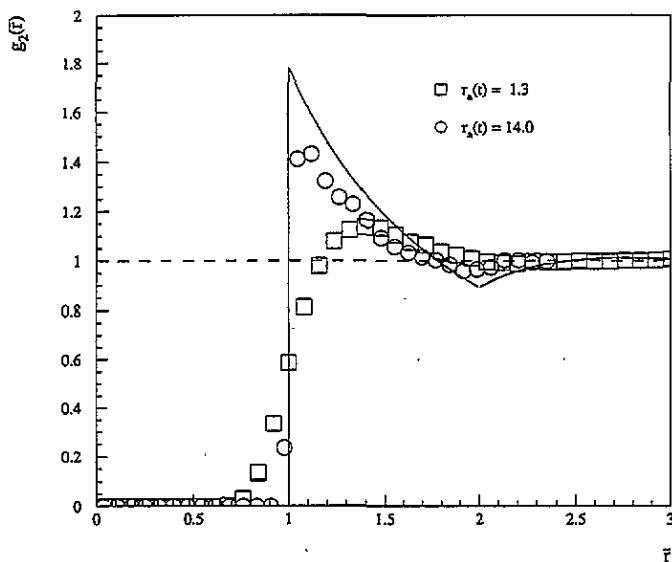


Figure 5. Pair correlation functions for the continuous SA model in two dimensions, as a function of the rescaled variable $\bar{r} = r/r_a(t)$. Errors are of the order of the symbol size. The smooth curve is the asymptotic limit in $d = 1$ for comparison. The value of r_0 is $1/\ln(100)$ and the initial density is 1.0

In two dimensions the previous remarks set an upper bound for the density, the inverse of the particle excluded volume or $\pi/2\sqrt{3}r_a^2(t)$ for close packing. A more realistic estimate of the particle density may be obtained from equation (3.3), by representing the excluded volume as a step in $g_2(r)$, i.e. $g_2(r, t) = \Theta(r - r_a(t))$, or even the two-particle approximation $g_2(r, t) = \exp(-w(r, t))$. In the latter case, background particles are seen by only one member of a pair at a time [6]. In both these cases, the asymptotic form of the density is

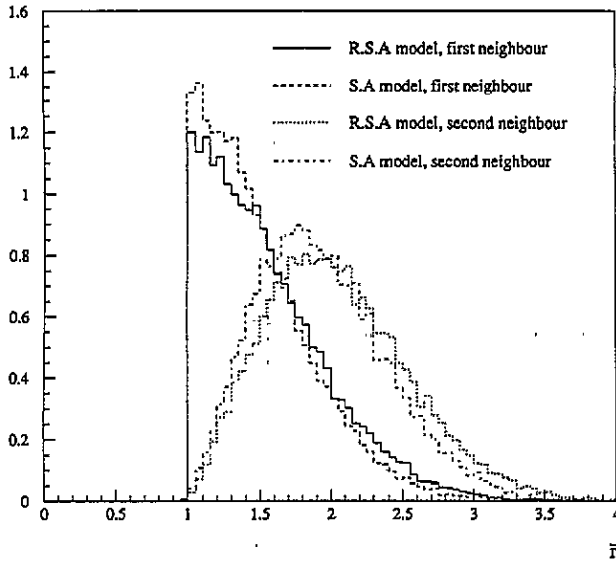


Figure 6. Comparison of the distributions of distances to first and second neighbours of particles surviving the annihilation process (SA model) and of the random deposition of non-overlapping disks at the same density (RSA). The parameters are as in figure 5.

easily found to be $\rho(t) = 1/\pi r_a^2(t)$. This approximation is still an over-estimation of the density (see [6]) showing that the true $g_2(r, t)$ must be greater than unity at the reaction front, cf figures 1 and 3 for dimension $d = 1$ and [6] for $d = 3$. For completeness, figure 5 shows $g_2(\bar{r}, t)$ in dimension $d = 2$. As in the static $A + B \rightarrow 0$ problem [3] there are correlations of length r_a , but in this case there is some additional structure shown by the oscillation of the correlation function. In the former case, the reaction simply reveals fluctuations in the initial distribution of A and B particles, leading to monotonic correlation functions [3]. The like-particle correlation functions deviate from unity because there is, in general, an imbalance of the numbers of A s and B s in a region of linear size $r_a(t)$, while the cross-correlation shows a simple excluded volume effect. In the case $A + A \rightarrow 0$, the initial state is, in contrast, increasingly homogenous on larger and larger scales. It is therefore reasonable to talk of ordering induced by the reaction, in view of the non-monotonic behaviour of the two-particle correlation function.

As in the one-dimensional case, this non-trivial behaviour determines the tail of the surviving particle density, $\rho(t)$. In any dimension d , relation (3.3) is valid with $\bar{g}_2(t) = \int dr w(|r|)g_2(r, t)$. When r_0 is sufficiently small, the integrand is sharply peaked at the reaction front and

$$\bar{g}_2(t) \sim g_\infty(\bar{r} = 1) \frac{d\pi^{d/2}}{\Gamma(1 + d/2)} r_0 w(r_a(t)) r_a^{d-1}(t)$$

yielding

$$\rho^{-1}(t) \sim g_\infty(\bar{r} = 1) \frac{\pi^{d/2}}{\Gamma(1 + d/2)} r_a^d(t).$$

The dynamical constant $g_\infty(\bar{r} = 1)$ is expected to depend upon the dimension only, and, in principle, can be evaluated through the SSA model in dimension d . This model cannot be exactly solved as the one-dimensional screening property is no longer valid. An MF-like

approximation of SSA can be obtained assuming the factorization of the pair probabilities, which is a reasonable assumption suggested by the random sequential deposition of dimers [12], which has dynamics very close to the SSA dynamics in any given stage. However, this is not a simple task and we do not perform it here. For the time being we give the numerical estimates found from MC experiments: $g_{\infty}(\bar{r} = 1) \sim 1.5\text{--}1.7$ for $d = 2$, and $g_{\infty}(\bar{r} = 1) \sim 1.4\text{--}1.6$ for $d = 3$ [6]. As for $d = 1$, $g_{\infty}(\bar{r} = 1) = e^{\nu} = 1.78107\dots$, it may be that g_{∞} is independent of dimension. Longer simulations are needed to check this.

To summarize, the distribution of surviving particles appears to be closely connected with the random deposition of non-overlapping objects (RSA) model. We observe that the equations governing the dynamics in each stage of the SSA model are similar to those in the RSA model. More empirically, figure 6 compares the distributions of first and second neighbours in the continuous SA model in $d = 2$ with the corresponding distribution for hard disks of diameter r_a at the same density. Except at the reaction front, where the exclusion of overlap is probabilistic rather than absolute in the SA model, the distributions are very close. We mention in passing that the angular distributions of the first and second neighbours are very similar.

5. Conclusion

We have defined a model—the SSA model—which can be exactly analysed in one dimension. The dynamical generation of the long-range order which is found can be compared, through a rescaling of the distance, to the short-range order due to volume exclusion found in RSA processes with some cooperative effects. We have shown that in the long-time limit this model and the SA models are related in a simple way. Our MC experiments and our analysis indicate that the SA model has essentially two regimes, which simplifies the description proposed in [6]. The short-time regime is MF-like. This regime ends when the reaction radius becomes comparable to the initial particle separation. Then, the dynamics develop in a way which can be described in terms of the SSA model though a suitable mapping of the parameters.

It would be interesting to consider the extension of the SSA model to the $A + B \rightarrow 0$ annihilation process. Here, the one-dimensional case can be analytically solved and may provide an accurate description of the asymptotics of the corresponding SA model to complement the existing numerical results [6, 13].

Acknowledgment

We thank Professor Yves Leroyer for his stimulating interest and for his collaboration in the early stage of this work.

References

- [1] Stengers I and Prigogine I 1984 *Order Out of Chaos* (London: Heinemann)
- [2] Bak P, Tang C and Wiesenfeld K 1987 *Phys. Rev. Lett.* **59** 381
- [3] Schnörer H, Kuzovkov V and Blumen A 1990 *J. Chem. Phys.* **92** 2310
- [4] Blumen A, Klafter J and Zumofen G 1986 *Optical Spectroscopy of Glasses* vol 1, ed Zschokke (Dordrecht: Reidel)
- [5] Kuzovkov V and Kotomin E 1988 *Rep. Prog. Phys.* **51** 1479
- [6] Brown R and Efremov N A 1991 *Chem. Phys.* **155** 357
- [7] Kulikov S G, Efremov N A, Personov R I and Romanovskii Yu V 1992 *Sov. Phys.—Solid State* **34** 1294
- [8] van Kampen N G 1981 *Int. J. Quantum Chem. (Quantum Chem. Symp.)* **16** 101

- [9] Kirkwood J G 1935 *J. Chem. Phys.* **3** 300
- [10] Tachiya M and Mozumder A 1974 *Chem. Phys. Lett.* **87**
- [11] Bonnier B, Boyer D and Viot P 1994 *J. Phys. A: Math. Gen.* **27** 3671
- [12] Evans J W 1993 *Rev. Mod. Phys.* **65** 1281
- [13] Schnörer H, Kuzovkov V and Blumen A 1989 *Phys. Rev. Lett.* **63** 805